Surface phonons on the NbC(001) and TaC(001) surfaces

S. Bağcı,[1] H. M. Tütüncü,[1] S. Duman,[1] and G. P. Srivastava[2]
[1]*Sakarya Üniversitesi, Fen-Edebiyat Fakültesi, Fizik Bölümü, 54187, Adapazarı, Turkey*
[2]*School of Physics, University of Exeter, Stocker Road, Exeter EX4 4QL, UK*
(Received 21 November 2011; revised manuscript received 31 January 2012; published 27 February 2012)

Structural, electronic, and vibrational properties of NbC(001) and TaC(001) are presented, based on the application of plane-wave basis, pseudopotentials, and the generalized gradient approximation of the density functional scheme. In agreement with previous theoretical and experimental studies, the rippled relaxation of these surfaces is observed. Both surfaces show metallic character due to a partially filled band. The calculated phonon-dispersion relations for both surfaces accord very well with the available experimental data. Energy locations and polarization characteristic of Rayleigh, Love, Wallis, Lucas, and Fuchs-Kliewer modes have been determined. Our results reveal that due to symmetry lowering the electron-phonon interaction on these surfaces is much weaker than the corresponding interaction in their bulk form.

DOI: 10.1103/PhysRevB.85.085437 PACS number(s): 63.20.dk, 68.35.Ja, 71.15.Mb, 74.25.Kc

I. INTRODUCTION

Refractory metal carbides have attracted a great deal of attention in the past 30 years since they are characterized by different degrees of covalent, ionic, and metallic bondings.[1] Consequently they exhibit interesting properties such as extremely high melting point, high hardness, high electrical conductivity, and superconductivity.[1] In addition to their bulk properties, surface properties of carbides have been studied due to their promise as surface catalysts.[2–4] So far two experimental techniques have been applied to obtain the structural properties of the (001) surfaces of NbC and TaC: low-energy electron diffraction (LEED) intensity analysis[5,6] and medium-energy ion scattering (MEIS).[7] These experimental studies show the primitive (1×1) structure but a marked rippling relaxation of the surface layer. On the theoretical side, Price *et al.*[8] reported a total-energy calculation of the relaxation of TaC(001), using a full-potential linear-combination-of-muffin-tin-orbitals electronic-structure method (LMTO). Following this theoretical work, a simple d-p tight binding model (TB) was proposed for the relaxation of the TaC(001) surface.[9] In addition to these two theoretical works, the rippled relaxation of these surfaces was examined using the first-principles molecular dynamics method.[10,11] A systematic study of the bulk and surface geometrical and electronic properties of a series of transition-metal carbides by the generalized gradient approximation was presented.[12]

In addition to their structural and electronic properties, phonon properties of transition-metal carbide surfaces must be studied because surface vibrations are involved in many processes on surfaces at ambient as well as elevated temperatures, such as surface diffusion, phase transitions on clean and adsorbate-covered surfaces, and desorption processes. In order to make theoretical studies of these processes it is essential first to obtain accurate dispersion curves surface phonon branches. Dispersion curves for a few optical and acoustical surface phonon branches for NbC(001) and TaC(001) have been determined along the $\overline{\Gamma}$–$\overline{M}$ symmetry direction on the surface Brillouin zone by angle-resolved high-resolution electron-energy-loss spectroscopy (EELS).[13,14] Up to now, surface phonon calculations for these surfaces have been performed using phenomenological shell model.[15,16] A simplified double-shell model method was used to obtain the phonon dispersion curves for the NbC(001) and TaC(001) surfaces by Lakshmi and Weber.[15] Following this theoretical work, Ishida and Terakura[16] investigated surface phonons on both surfaces using the double-shell model in a slab geometry. However, there are considerable difference between the double-shell model[16] and experimental results[13,14] with respect to the surface phonon modes lying in the acoustic-optical gap region. Moreover Ishida and Terakura[16] were not able to reproduce the highest surface optical branch in their calculations. Very recently we have presented surface phonon dispersion curves and density of states for the (001) surface of TiC and HfC using *ab initio* pseudopotential and a linear response scheme.[17,18] The calculated phonon dispersion curves for both surfaces agree very well with experimental data.[19,20] The success of our calculations can be related to a more rigorous treatment of the surface force constants and effective charges in the *ab initio* calculations.

In the present paper, we first present results of an *ab initio* plane-wave pseudopotential calculation for the relaxed atomic geometry and electronic structure of NbC(001) and TaC(001). The calculated atomic geometries of both surfaces are compared with available experimental[5–7] and theoretical results.[8–10,12] The surface electronic states on these surfaces are identified by comparing the surface electronic and projected bulk electronic spectrum. Phonon dispersion curves for both surfaces have been calculated using a linear-response approach based on density-functional theory. The calculated phonon dispersion curves for both surfaces fit very well with published experimental data.[13,14] The origins of various interesting phonon modes on these surfaces are explained clearly. We have also calculated the electron-phonon coupling parameter for the bulk and surface of these materials. Our results indicate that the superconductivity vanishes on the (001) surface, due to the weak electron-phonon interaction.

II. METHOD

We used the first-principles plane wave pseudopotential method based on the density functional theory. The electron-ion interaction was described by using ultrasoft pseudopotentials, which have been generated according to a modified Rappe-Rabe-Kaxiras Joannopolus scheme.[21] The

density functional theory has been implemented within the generalized gradient approximation (GGA), using the Perdew-Burke-Ernzerhof method.[22] The bulk phase of NbC and TaC is described in the rock-salt structure. The (001) surface of these materials was modified by employing the supercell technique, in which periodic boundary conditions are applied to a surface supercell including a slab of atomic layers and a vacuum region. Our supercell contained 26 atoms located in a slab of 13 atomic layers and a vacuum region equivalent of five atomic layers. For the **k**-point sampling, we used the $16 \times 16 \times 16$ Monkhorst-pack **k** mesh in the irreducible wedge of the Brillouin zone of the rock-salt structure and $20 \times 20 \times 1$ Monkhorst-pack **k** mesh in the irreducible part of the surface Brillouin zone. The electronic wave functions were expanded in terms of a basis set of plane waves, up to a kinetic-energy cutoff of 60 Ry, and the Kohn-Sham equations were solved using an iterative conjugate gradient scheme[23] to find the total energy and atomic forces. All atoms, except those in the middle of the slab, were then relaxed toward their optimum configuration following a conjugate gradient algoritm. The equilibrium positions are determined with numerical uncertainty of less than 0.01 Å, with all forces smaller than 0.1 mRy/a.u.

Phonon calculations were carried out by employing the density-functional perturbation theory and using the computer code Quantum Espresso.[24] Within this scheme, second-order derivatives of the total energy were calculated to obtain the dynamical matrix. A static linear response of the valence electrons was considered in terms of the variation of the external potential corresponding to periodic displacements of the atoms in the supercell. The screening of the electronic system in response to the displacement of the atoms was taken into account in a self-consistent manner. In order to obtain the force constants matrices for bulk NbC and TaC, and to carry out the inverse Fourier transformation, we used **q** points on a $8 \times 8 \times 8$ mesh. For surface phonon calculations, six dynamical matrices were calculated corresponding to a $4 \times 4 \times 1$ **q** points mesh within the irreducible segment of the surface Brillouin zone. Then two-dimensional Fourier interpolation was made to obtain surface phonon dispersion curves as well as phonon density of states. The technique for the calculation of electron-phonon coupling has been described in detail in our previous works.[25] Fermi-surface sampling for the evaluation of the electron-phonon matrix elements was done using $40 \times 40 \times 1$ **k** mesh with Gaussian width $\sigma = 0.02$ Ry. The electron-phonon mass enhancement parameter (λ) is obtained as

$$\lambda = \sum_{\mathbf{q}j} \lambda_{\mathbf{q}j} W(\mathbf{q}), \tag{1}$$

where $W(\mathbf{q})$ is the weight of the $\boldsymbol{q}$th special phonon wave vector. The above summation has been done over the surface phonon modes.

III. RESULTS

A. Atomic geometry and electronic structure

Before starting the surface calculations, we optimized the rock-salt structure of these materials. The lattice parameters

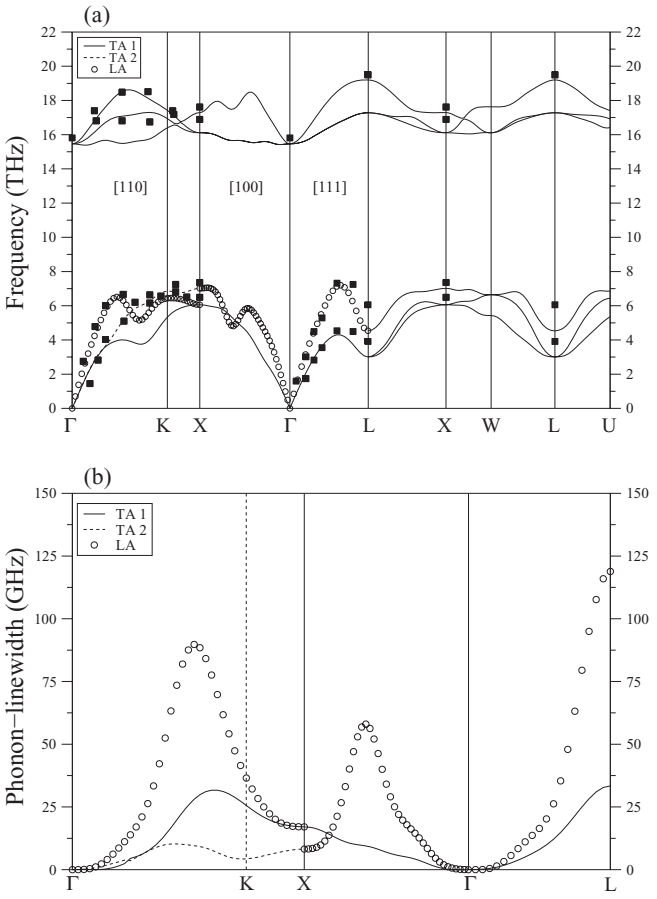

FIG. 1. (a) The calculated phonon spectrum of NbC. Experimental data[27] are denoted by filled squares. (b) Phonon line width for acoustic phonon branches in NbC. In the [100] and [111] directions, the two transverse modes are degenerate.

are found to be 4.487 Å for NbC and 4.464 Å for TaC, which agree well with their experimental values of 4.471 and 4.456 Å.[26] These lattice constant values were used in our surface calculations. In order to show the success of the application of the density-functional perturbation theory, the phonon dispersion curves of NbC along the several symmetry directions are compared with experimental data[27] in Fig. 1(a). As can be seen from this figure, the calculated results accord very well with previously published experimental results.[27] Similar agreement has also been found for the phonon spectrum of TaC. A striking feature of the phonon spectrum for NbC is that the longitudinal acoustic (LA) branch becomes very soft along all the three principal symmetry directions [100] (Γ–X), [110] (Γ–K), and [111] (Γ–L). Along [100] and [110] the LA branch acquires a "dip," with frequency lower than the transverse acoustic (TA) branch. In addition to this, the lower TA branch becomes soft along the [110] and [111] directions. Thus, the lower TA branch acquires a "dip" at the L point. In order to establish a correlation between the anomalous phonon dispersion and electron-phonon interaction, we have also presented the phonon line width for TA and LA modes in Fig. 1(b). Although the LA branch lies below the TA branches in the phonon spectrum, the phonon line width for the LA branch lies above the phonon line widths for the TA branches,

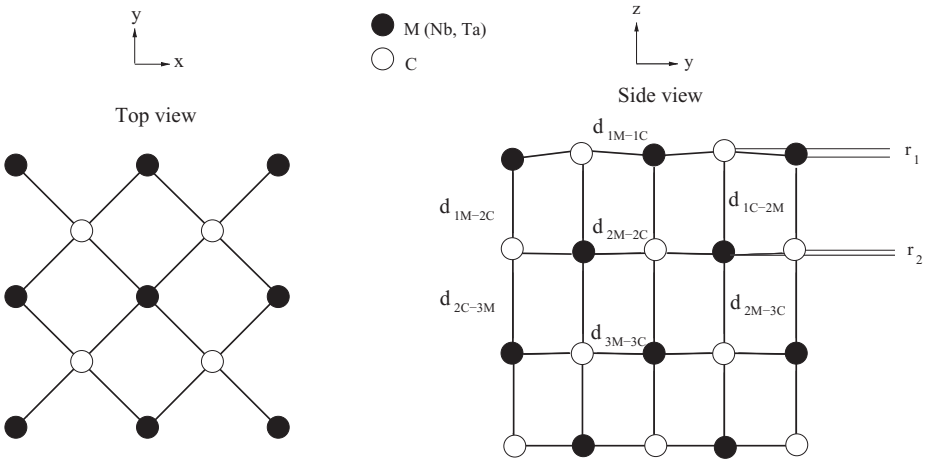

FIG. 2. The relaxed top and side views of the MC(001) surface. The bond lengths and rumplings are indicated in the side view of the MC(001) surface.

signaling a much larger electron-phonon interaction in the LA branch. The most notable feature is that LA phonon line width reaches a peak value of 118 GHz at the L point.

The (001) face of transition metal carbides retains its primitive 1×1 periodicity and is nonpolar, including an equal number of transition metals and carbon atoms on each surface layer. In order to find minimum energy, at the surface layer the metal atoms move away from the bulk while the carbon atoms move into bulk. The relative displacement of the surface layer metal and carbon atoms defines a measure of the amount of surface rippling (r_1), which mainly characterizes the relaxation of the surface. The metal and carbon atoms in the subsurface layer show a similar relaxation; i.e., metal atoms (carbon atoms) move away (toward) the bulk, *albeit* on a much smaller scale. Price *et al.*[28] found that the truncated bulk electric fields correctly indicate the direction of relaxation, and that the primary cause of the carbon-out, metal-in surface layer relaxation is the electric field of the underlying bulk material. We label the vertical separation between the second layer atoms r_2. The key structural parameters and bond lengths are shown in Fig. 2. Table I summarizes our calculated results for the relaxation parameters of the surfaces, with previously available experimental[5–7] and theoretical results.[8–12] In general, our calculated structural parameters accord very well with the previously reported theoretical and experimental values. We note that the surface bond lengths for both surfaces are smaller (by up to 4%) than the bulk bond lengths. The calculated value of r_1 for the TaC(001) surface is equal to the experimental value of 0.20 Å.[5] Additionally, the calculated bond-length values for d_{1Nb-2C}, d_{1C-2Nb}, d_{2Nb-3C}, and d_{2C-3Nb} also compare very well with their corresponding previously reported GGA values of 2.10, 2.33, 2.25, and 2.27 Å.[12] In previous experimental studies,[5,7] the surface relaxation on transition metal carbides surfaces has been explained in terms of ϵ (surface relaxation) and $\delta\epsilon$ (surface rumpling) parameters, which are given by

$$\epsilon = (\delta_C + \delta_M)/2d \times 100(\%),$$
$$\Delta\epsilon = (\delta_C - \delta_M)/d \times 100(\%).$$

Here d is the bulk interplanar distance, and δ_C and δ_M are displacements of the top layer carbon and transition metal atoms toward the vacuum side, respectively. Our calculated values for ϵ and $\delta\epsilon$ are also listed in Table I. As can be seen from this table, our calculated values of these quantities for both surfaces compare very well with the FPMD and previous GGA values.[10,12] Excellent agreement has also been found between our results and experimental results[5] for these quantities.

Figure 3 presents the electronic structure of the NbC(001) and TaC(001) surfaces with their projected bulk band structures (shaded in gray). The general pattern of the electronic structure of these surfaces is very similar to each other. We have

TABLE I. Vertical buckling of top two layers (r_1 and r_2) and the calculated bond lengths (d_{M-C}, M = Nb and Ta), compared with previous experimental and theoretical results. Units: Å.

Source	r_1	r_2	d_{1M-1C}	d_{2M-2C}	d_{3M-3C}	d_{1M-2C}	d_{1C-2M}	d_{2M-3C}	d_{2C-3M}	ϵ	$\Delta\epsilon$
NbC(001)	0.182	0.077	2.251	2.245	2.244	2.072	2.330	2.225	2.258	−1.4	8.1
LEED[6]	0.160										
GGA[12]	0.180	0.050				2.100	2.330	2.250	2.270		8.0
FPMD[11]	0.220	0.078								−1.2	9.6
TaC(001)	0.200	0.076	2.241	2.233	2.232	2.073	2.350	2.210	2.234	−0.8	9.0
LEED[5]	0.200	0.040								−0.7	9.0
MEIS[7]										1.4 ± 0.3	4.9 ± 0.5
GGA[12]	0.200	0.050				2.090	2.340	2.230	2.250		8.9
TBM[9]	0.120	0.090									
FPMD[10]	0.230									−0.6	10.6
LMTO[8]										1.1	9.4
FPMD[11]										−0.8	10.3

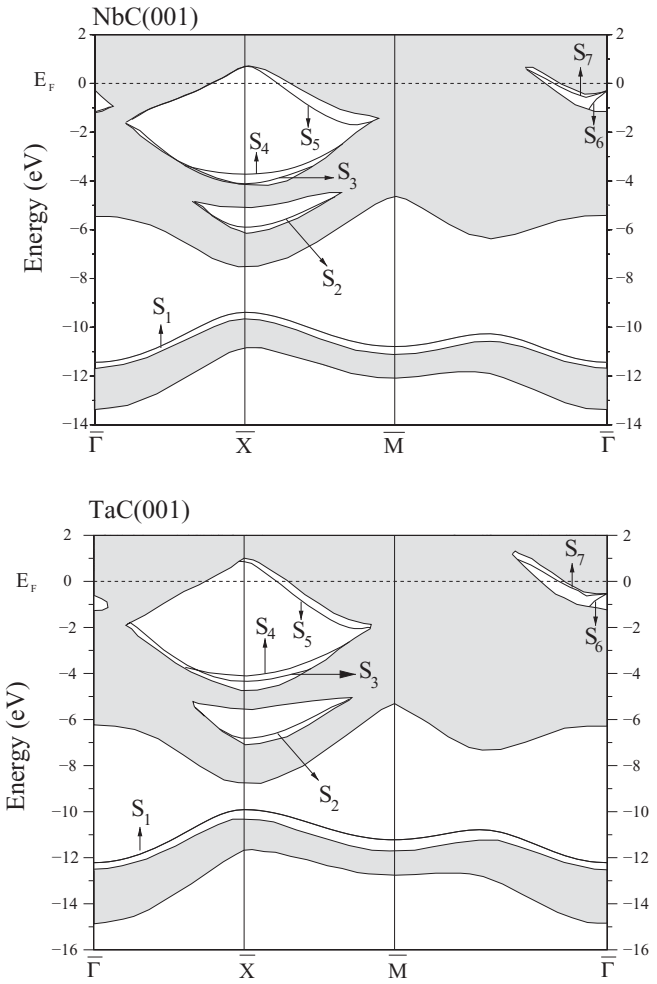

FIG. 3. The electronic structure of the NbC(001) and TaC(001) surfaces. The projected bulk spectrum is shown by the gray area.

found several gap regions in their electronic band structure. Only truly localized surface states lie in these gap regions. As can be seen from this figure, we have identified a total of seven surface states on the both surfaces. Only two of them (S_5 and S_7) cross the Fermi level along the $\overline{X}$–$\overline{M}$ and $\overline{M}$–$\overline{\Gamma}$ directions, respectively. This feature clearly indicates the metallic nature of both surfaces. A similar observation has been made in previous theoretical studies.[11,17,18]

B. Surface phonons and electron-phonon interaction

Because of the presence of two surfaces in the slab, the surface modes occur in pairs. However, in our calculations, the energy difference between these surface phonon pairs is less then 0.1 meV. This difference is less then experimental error margin, which is around 1 meV. Thus, we will discuss only one of them in this subsection. The surface phonon dispersion curves for the NbC(001) surface are shown in Fig. 4 along the three symmetry directions in the two-dimensional Brillouin zone. The shaded areas are the projection of the bulk phonon bands. The localized surface phonon modes are shown by thick lines, and the results from the EELS measurements[13,14] along the symmetry direction $\overline{\Gamma}$–$\overline{M}$ are shown by filled squares. Note that many of the surface states become resonant with

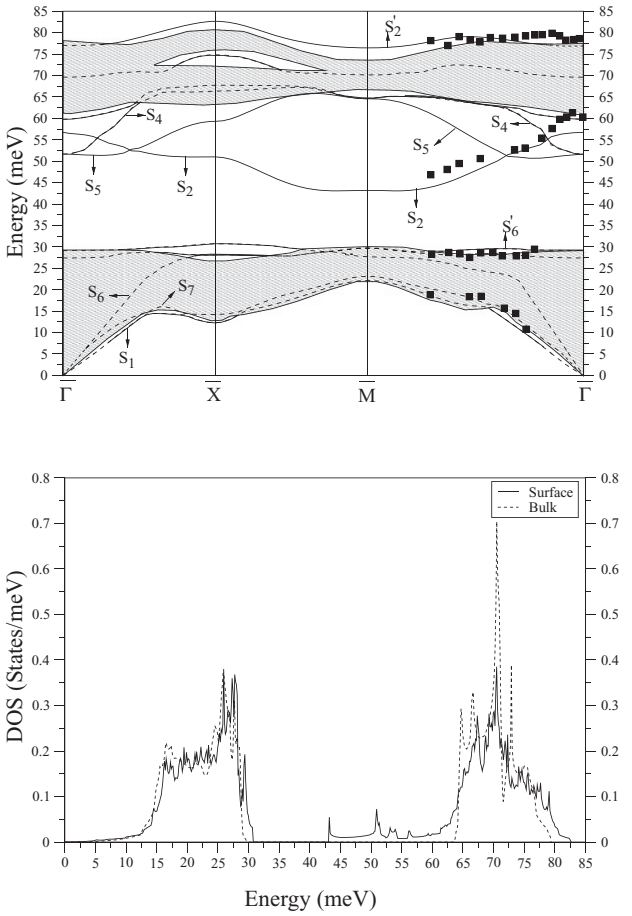

FIG. 4. Dispersion of phonon modes and density of states (DOS) on the NbC(001)(1 × 1) surface obtained from the GGA calculation. The localized surface phonon modes are shown by solid lines; the resonant surface phonon modes are plotted with dashed lines; EELS measurements[13,14] are shown by filled squares. The bulk results are shown by the hatched region for the dispersion curve and dashed lines for the density of states.

bulk bands, and their exact energy locations are difficult to determine. By examining the surface dominance of the corresponding atomic displacement we have made a rather tentative judgment on their dispersion within the bulk projected region. The resonant modes are plotted with dashed lines.

For the surfaces studied here, we have identified, as expected, up to 12 surface modes corresponding to vibrations of atoms in the top two layers. Three of these are surface acoustic modes, and the rest of them are surface optical modes. We first briefly discuss the agreement between our results and experimental results. In general, our results accord very well with experimental data.[13,14] In particular, the agreement between the experimental[13,14] and our GGA results for the highest optical phonon branch is an excellent. It is significant to note that this phonon branch was not observed in previous shell model calculations.[16] As a result of the large mass difference between Nb and C, a significant gap between acoustic and optical bulk branches exists. Up to four pure surface phonon modes appear throughout the surface Brillouin zone (SBZ) in this gap region. The lowest one with an energy of 29 meV is

nearly flat throughout the SBZ. There is a sharp phonon peak at 29 meV in the phonon density of states due to the flatness of this pure surface phonon mode. The other gap phonon modes show a considerable dispersion throughout the SBZ. Due to the dispersion of these gap phonon modes, several small peaks (between 42 and 60 meV) lie in the phonon density of states for the NbC(001) surface. Different from previous theoretical calculations,[16] all pure surface phonon modes obtained in our work compare very well with experimental results along the $\overline{\Gamma}$–$\overline{M}$ symmetry direction. As a result, we can say that our GGA calculations predict the localization of gap phonon modes much better than the previous shell model calculations[16] did. The reason for this difference is that in using bulk interaction models for surface calculations, as implicitly done in previous shell model calculations, there is always the question as to what extent this is a valid procedure. Bulk interaction models, because of the bulk symmetry they represent, contain implicitly a number of simplifications, cancellations, or even two-body parametrization of many-body interactions, which cannot be represented in such a way at the surface because of the breaking of bulk symmetry at the surface. We also note that in contrast to the phonon dispersion curves of TiC(001) and HfC(001),[17,18] there is no stomach gap region for the phonon spectrum of NbC(001) in the bulk acoustic phonons region because the bulk LA branch crosses the TA branch along the Γ–K and Γ–X bulk symmetry directions [which can clearly be seen in Fig. 1(a)]. The calculated surface acoustic phonons are also in good agreement with the experimental measurements along the $\overline{\Gamma}$–$\overline{M}$ direction.

When the wave vector lies along the $\overline{\Gamma}$–$\overline{X}$ and $\overline{\Gamma}$–$\overline{M}$ axes, there is a mirror reflection symmetry about the plane that contains the surface normal and the wave vector. Thus, the vibration is separated into a saggital-plane (SP) mode, which oscillates in the plane, and shear horizontal (SH) mode, whose eigenvector is vertical to plane. Only the SP mode is observable by EELS. Let us consider only the vibration topmost layer at the $\overline{\Gamma}$ point. There are six modes corresponding to the freedom of the two atoms in the surface unit cell. Three acoustical modes have zero vibrational energies, and optical ones are S_2, S_4, and S_5 (see Fig. 4). We now explain the character of these three modes. The eigenvector of S_2 is mostly localized with the z component of the top-layer carbon atoms, and thus the character of this phonon mode is SP. It is called the Wallis mode on the (001) surface of the rock-salt structure. As can be seen from Fig. 4, S_2 crosses S_4 and S_5 along the $\overline{\Gamma}$–$\overline{X}$ and $\overline{\Gamma}$–$\overline{M}$ symmetry directions. S_4 and S_5 are the Lucas modes and are mostly produced by the oscillation of top-layer carbon atoms parallel to the surface. The C_{4v} point-group symmetry requires the degeneracy of two Lucas modes (S_4 and S_5) at both the $\overline{\Gamma}$ and $\overline{M}$ points. The polarization of S_4 is SP, and that of S_5 is SH. The surface modes are classified according to the bulk bands from which they derive and according to their additional physical characteristics. The Lucas modes are peeled off from the bottom of the transverse optical (TO) bulk bands, and the Wallis mode is peeled off from the longitudinal optical (LO) band. Due to a large band gap region, S_2, S_4, and S_5 exist as pure surface modes throughout the SBZ. As $\mathbf{q}$ is increased from zero, along the $\overline{\Gamma}$–$\overline{X}$ direction, mode S_4 mixes with the surrounding bulk optical modes and becomes pseudosurface mode. However, S_2 and S_5 are rigorously decoupled from the surrounding bulk modes, so they both persist as pure surface modes in the both symmetry directions. S_2, S_4, and S_5 are the only microscopic surface modes existing for $\mathbf{q} = 0$. This means that that their localization is always confined to within a few layers from the surface. Away from the zone center, surface acoustic frequencies are different from zero. The acoustic frequencies are labeled S_1, S_7, and S_6, respectively. Along the $\overline{\Gamma}$–$\overline{M}$ direction, S_1 is the Rayleigh surface wave. It is peeled down from the bottom edge of the TA bulk bands by perturbation imposed on the dynamics of the bulk crystal by the free-surface condition. This phonon mode has SP polarization character. S_7 (Love mode) is the acoustic surface phonon, which also peels off from the TA phonon band. It is formed by the oscillation of metal atoms vertical to the saggital plane. These TA surface modes are examples of macroscopic modes, which means that their surface localization diminishes (penetration depth increases) with increasing wave lengths ($\mathbf{q} \to 0$) and disappear at $\overline{\Gamma}$. Thus, these modes also include atomic vibration from bulk atoms when $\mathbf{q}$ goes to zero. As a result, it is very difficult to identify them close to the zone center. Thus, we have shown these phonon modes with dashed lines close to the zone center in Fig. 4.

In the long-wavelength limit these modes are also found in continuum theory. It is important to note that these phonon modes switch their polarization characters along the $\overline{\Gamma}$–$\overline{X}$ direction. A similar observation has been made for surface phonon calculations on the (001) surfaces of TiC and HfC.[17,18] S_6 is a microscopic acoustic surface mode peeled down from the LA subband. For the HfC(001) and TiC(001) surfaces,[17,18] it appears in the LA–TA gap along the zone boundary $\overline{X}$–$\overline{M}$. However, the prediction of the appearance of S_6 becomes very different for the NbC(001) surfaces because of the strong overlap of the LA and TA bulk bands in bulk NbC. In order to obtain other phonon modes in Fig. 4, we have to consider the vibrations of second-layer atoms as well. Hence, the S_2' (Fuchs-Kliewer branch) mode should come from the freedom of the inner atomic layers such as the second or third layers. The high vibrational energy of S_2' indicates that the carbon is dominant in this mode. The polarization of the S_2' mode is purely perpendicular to the surface at the $\overline{\Gamma}$ point. A similar observation has been made for the (001) surface of TiC and HfC.[17,18] Finally, S_6' has a polarization vector vertical to the surface. S_6' mode is mainly localized on the second layer metal atoms. Finally, note that there are two branches between S_2' and S_4. These branches have SP character with the vibrations of second-layer C atoms.

The calculated phonon dispersion curves and density of states for the TaC(001) surface are illustrated in Fig. 5. Our surface phonon results on this surface are in very good agreement with experimental results[13,14] along the symmetry directions $\overline{\Gamma}$–$\overline{X}$ and $\overline{\Gamma}$–$\overline{M}$. In general, the surface phonon spectra of this surface are very similar to that of NbC(001). However, differences have been observed between the phonon dispersion curves of these surfaces. First, the S_2' branch always lies above the bulk optical phonons for the (001) surface of TaC. Second, the S_2 branch of the TaC(001) surface always lies below the S_4 and S_5 branches of this surface. Finally, the S_1 and S_7 branches of TaC(001) surface fall below the bulk acoustic continuum and become truly localized along the $\overline{\Gamma}$–$\overline{X}$ and the $\overline{\Gamma}$–$\overline{M}$ directions.

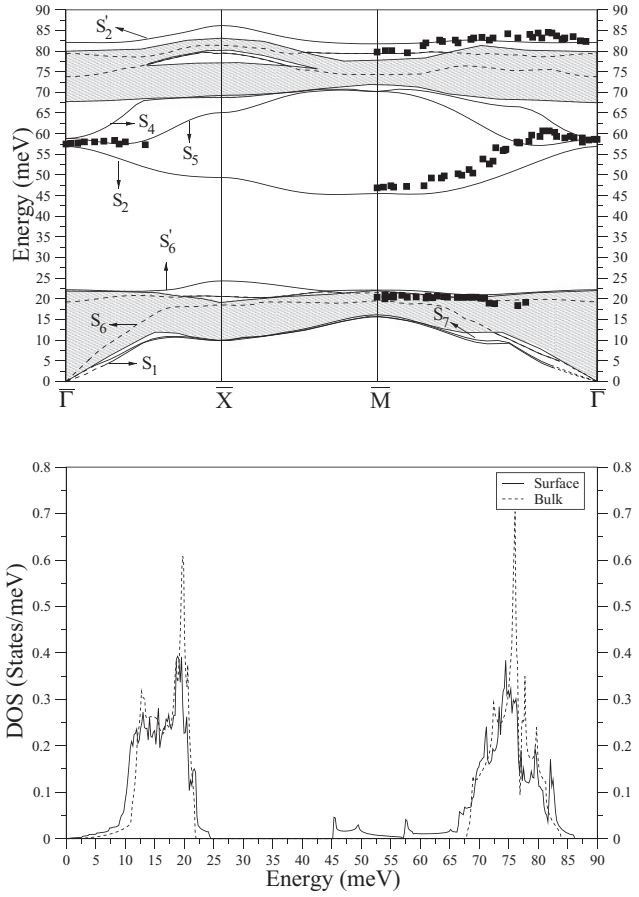

FIG. 5. Surface phonon modes and density of states on the TaC(001)(1 × 1) surface. The localized surface phonon modes are shown by solid lines; the resonant surface phonon modes are plotted with dashed lines; EELS measurements[13,14] are shown by filled squares. The bulk results are shown by the hatched region for the dispersion curve and dashed lines for the density of states.

As can be seen from Figs. 4 and 5, we have not observed strong phonon anomalies (dips) for NbC(001) and TaC(001) surfaces. This picture is very different from their bulk phonon dispersion curves [for example, see Fig. 1(b) for NbC]. The total electron-phonon coupling parameter is found to be 0.12 and 0.11 for the NbC(001) and TaC(001) surfaces, respectively. These values are much smaller than our calculated bulk values of 0.88 (NbC) and 0.75 (TaC). Thus, our electron-phonon interaction calculations indicate that electron-phonon interaction on the (001) surface of NbC and TaC is much weaker than the corresponding interaction in their bulk forms. We strongly believe that the much weaker surface electron-phonon interaction results from reduction in symmetry.

IV. SUMMARY

In this paper the atomic geometry and electronic structure of the (001) surface of NbC and TaC were investigated and discussed by employing an *ab initio* pseudopotential theory. Following these calculations, we calculated the vibrational properties of these surfaces by applying the *ab initio* linear response approach to our relaxed atomic geometries. Our work supports the relaxed (1 × 1) structure of these surfaces, with the rumpling parameter r_1 for TaC(001) in agreement with previously reported LEED and MEIS analyses, and first-principles molecular dynamics calculations.

The calculated surface phonon dispersion curves for both surfaces fit very well with angle-resolved high-resolution electron-energy-loss spectroscopy results. We have discussed energy locations and polarization characteristic of Rayleigh, Love, Wallis, Lucas, and Fuchs-Kliewer modes in detail. In contrast to a previous shell model calculation, our work predicts clear existence of gap phonon modes as well as a surface branch above the bulk spectrum.

A detailed comparison of bulk and surface phonon dispersion curves suggests that phonon anomalies (dips) are reduced for NbC(001) and TaC(001) surfaces. This has resulted in the total electron-phonon coupling parameter λ to be much reduced for these surfaces [0.12 for NbC(001) and 0.11 for TaC(001)] compared to the corresponding bulk values of 0.88 and 0.75, respectively. We believe that this large difference comes from the breaking of bulk symmetry at the surface. In order to confirm our present belief, we suggest that similar detailed investigations of phonons be undertaken on transition metal carbide surfaces and transition metal nitride surfaces.

ACKNOWLEDGMENTS

This work was supported by the Scientific and Technical Research Council of Turkey (TUBİTAK, Grant No. 108T542). The calculations were performed using the Intel Nehalem (i7) cluster (ceres) at the University of Exeter.

[1]L. E. Toth, *Transition Metal Carbides and Nitrides* (Academic, New York, 1971).
[2]I. Kojima, E. Miyazaki, Y. Ione, and I. Yasumori, J. Catal. **59**, 472 (1979).
[3]S. T. Oyama and G. L. Haller, Catalysis **5**, 333 (1982).
[4]M. Orita, I. Kojima, and E. Miyazaki, Bull. Chem. Soc. Jpn. **59**, 689 (1989).
[5]G. R. Gruzalski, D. M. Zehner, J. R. Nonnan, H. L. Davis, R. A. Didio, and K. Müller, J. Vac. Sci. Technol. A **7**, 2054 (1989).
[6]M. Tagawa, M. Okuzawa, T. Kawasaki, C. Oshima, S. Otani, and A. Nagashima, Phys. Rev. B **63**, 073407 (2001).
[7]Y. Kido, T. Nishimura, Y. Hoshino, S. Otani, and R. Souda, Phys. Rev. B **61**, 1748 (2000).
[8]D. L. Price, J. M. Wills, and B. R. Cooper, Phys. Rev. B **48**, 15301 (1993).
[9]K. E. Tan, A. P. Horsfield, D. N. Manh, D. G. Pettifor, and A. P. Sutton, Phys. Rev. Lett. **76**, 90 (1996).
[10]K. Kobayashi, Jpn. J. Appl. Phys. Part 1 **39**, 4311 (2000).

[11]K. Kobayashi, Surf. Sci. **493**, 665 (2001).
[12]F. Vines, C. Sousa, P. Liu, J. A. Rodriguez, and F. Illas, J. Chem. Phys. **122**, 174709 (2005).
[13]C. Oshima, R. Souda, M. Aono, S. Otani, and Y. Ishizawa, Phys. Rev. Lett. **56**, 240 (1986).
[14]C. Oshima, R. Souda, M. Aono, S. Otani, and Y. Ishizawa, Solid State Commun. **57**, 283 (1986).
[15]G. Lakshmi and W. Weber, Verh. Dtsch. Phys. Ges. (VI) **10**, 617 (1975).
[16]H. Ishida and K. Terakura, Phys. Rev. B **34**, 5719 (1986).
[17]S. Bağcı, T. Kamış, H. M. Tütüncü, and G. P. Srivastava, Phys. Rev. B **80**, 035405 (2009).
[18]T. Kamış, S. Bağcı, H. M. Tütücü, S. Duman, and G. P. Srivastava, Philos. Mag. **91**, 946 (2011).
[19]C. Oshima, T. Aizawa, M. Wuttig, R. Souda, S. Otani, Y. Ishizawa, H. Ishida, and K. Terakura, Phys. Rev. B **36**, 7510 (1987).
[20]M. Wuttig, C. Oshima, T. Aizawa, R. Souda, S. Otani, and Y. Ishizawa, Surf. Sci. Lett. **192**, 575 (1987).
[21]A. M. Rappe, K. M. Rabe, E. Kaxiras, and J. D. Joannopoulos, Phys. Rev. B **41**, 1227 (1990).
[22]J. P. Perdew, K. Burke, and M. Ernzerhof, Phys. Rev. Lett. **77**, 3865 (1996).
[23]A. Umerski and G. P. Srivastava, Phys. Rev. B **51**, 2334 (1995).
[24]P. Giannozzi *et al.*, J. Phys. Condens. Matter **21**, 395502 (2009).
[25]H. M. Tütüncü and G. P. Srivastava, J. Phys. Condens. Matter **18**, 11089 (2006).
[26]A. M. Nartowski, I. P. Parkin, M. MacKenzie, A. J. Craven, and I. MacLeod, J. Mater. Chem. **9**, 1275 (1999).
[27]H. G. Smith and W. Gläser, in *Proceedings of the International Conference on Phonons, Rennes*, edited by M. A. Nusimovici (Flammarion, Paris, 1971), p. 145.
[28]D. L. Price, J. M. Wills, and B. R. Cooper, Phys. Rev. Lett. **77**, 3375 (1996).